Advanced modelling of runoff and soil redistribution for agricultural systems: the SERT model

M. López-Vicente [a, *], A. Navas [a], L. Gaspar [b], J. Machín [a]

[a] *Department of Soil and Water, Estación Experimental de Aula Dei, EEAD–CSIC. Avda. Montañana 1005, 50059 Zaragoza, Spain*

[b] *Cranfield University, Cranfield Water Sciences Institute, Cranfield, Bedfordshire MK43 0AL, United Kingdom*

[*] *Corresponding author. E-mail: mvicente@eead.csic.es*

Submitted	15 October 2012
Submitted in revised form - 1	18 March 2013
Submitted in revised form - 2	30 March 2013
Accepted for publication	**2 April 2013 → DOI:10.1016/j.agwat.2013.04.002**

Published in *Agricultural Water Management* **125**: 1-12 (Issue July 2013) – Available since 7 May 2013

Abstract

Hydrological and soil erosion models allow mapping and quantifying rates of runoff depths and soil redistribution for different land uses and climatic scenarios. Mediterranean soils are threatened by marked seasonal changes in the climatic, thus soil and vegetation parameters and modelling predictions at monthly scale are required. The semi-physically-based Soil Erosion and Redistribution Tool (*SERT*) model is presented together with the results of its application in a Mediterranean agro-ecosystem (NE Spain) with a detailed database. The hydrological module is based on the recently published *DR2* (Distributed Rainfall-Runoff) water balance model and the effects of man-made infrastructures on the natural dynamics of runoff connectivity are added. The erosion module is built using, as the basis, the Revised Morgan, Morgan and Finney model, and the new Remaining runoff Transport Capacity (TC_r) factor used to estimate the rates of soil loss and deposition. Predicted runoff depth varied in time and space, presenting areas without runoff production mainly in Rendzic Leptosols and Haplic Calcisols between November and April. Average soil erosion was high in cultivated and bare soils, ca. 20 and 10 Mg ha^{-1} yr^{-1}, whereas rangeland soils were affected by moderate and, in some areas, by limited erosion processes. Soil erosion was minimal in February (0.08 Mg ha^{-1} month^{-1} on average) and 23 times higher in October. The *SERT* model allowed mapping the significant changes in the monthly values of soil redistribution quantifying the variability in the magnitude of the processes involved. Predicted values of average soil loss and deposition were validated against quantified values with ^{137}Cs obtaining an average

Nash–Sutcliffe efficiency of 0.48 (Pearson's r = 0.709) and a sediment balance of -1.15 Mg yr^{-1} for the whole catchment that is consistent with the karst processes of the study area. The new model is an easy-to-run, reliable, low-input-demanding management tool with valuable outputs for hydrological and soil erosion studies in small agricultural catchments.

Keywords: DR2 model; Cumulative runoff; SERT model; Soil redistribution; Agricultural system; ^{137}Cs

1. Introduction

Soil erosion by water is a widespread problem throughout the world that causes the loss of fertile soil and crop yield in agricultural areas and a reduction in the overall quality and functions of the soils (Pimentel, 2000; Stavi and Lal, 2011). The current average erosion rates are a factor of 12 higher than soil sustainability, on the basis of the average rate of soil formation (Pimentel et al., 1999), and also the social and economic costs of erosion remain high due to the on-site and off-site consequences (e.g. Diao and Sarpong, 2011; Rivera et al., 2011). Accurate studies and measurements and sustainable land management are the keys to reduce agricultural soil loss. However, surface runoff, soil detachment and sediment delivery are non-linear processes that depend on many soil, climatic, topographic, vegetation and land use parameters and, furthermore, their effects change when considering different temporal and spatial scales (Cerdà et al., 2013). Hydrologic and soil erosion processes also vary as a function of the conditions prior to a rainfall event (De Baets et al., 2011) and of the magnitude of the erosion process itself (Gonzalez-Hidalgo et al., 2010). Moreover, human activities have been transforming the landscape since the first settlements, the creation of agricultural lands and the overexploitation of forests (García-Ruiz, 2010) accelerating and triggering in some places the processes of soil loss and degradation. As a consequence of these activities, numerous linear landscape elements (unpaved and paved trails, roads, land levelling, irrigation ditches, stone walls, dams, etc.) appear in landscapes, modifying the patterns of the overland flow and sediment connectivity.

Modelling hydrology and soil erosion is a difficult task to perform accurately in terms of time, space and rates due to its great complexity and the many factors involved. Initial attempts were carried out as empirical equations for small or limited areas (e.g. plots, fields and hillslopes). The studies of Mockus (1949) and Andrews (1954) constituted the building blocks of the Soil Conservation Service – runoff Curve Number (*SCS-CN*) (SCS-USDA, 1985) that has been successfully used in many environments and even incorporated in one of the most ambitious and currently used models, the Soil and Water Assessment Tool (*SWAT*; Arnold et al., 1998). The studies on plots undertaken by Wischmeier and Smith (1958 and 1978) regarding the relationship between rainfall energy, soil erodibility and soil loss as well as the development of the Universal Soil Loss Equation (*USLE*), yield the basis for the well-known *RUSLE* model (Renard et al., 1991), that has been one of the most studied and most used predictive models for rill and interrill soil erosion by water. An adapted version of the *RUSLE* equation is the *WATEM/SEDEM* (Van Rompaey et al., 2001) model that predicts spatially distributed rates of annual soil loss and deposition at catchment scale and also estimates tillage erosion. Other models have been developed to simulate not only surface runoff and soil erosion processes but also nutrient, pollutant and sediment delivery and deposition processes, such as the *CREAMS* (Kinsel, 1980) and *AGNPS* (Young et al., 1987) models.

Other available models are the expert-based *STREAM* (Cerdan et al., 2002) and the distributed split-parameter *TETIS* (Francés et al., 2007) hydrological models, and the dynamic *LISEM* (De Roo et al., 1995) model of soil erosion. All these models are integrated and run with GIS techniques and in some cases offer the possibility of being downloaded as executable files, as is the case of the empirical *RUSLE2* (Foster et al., 2000), the process-based *WEPP* (Adams et al., 2012), the complex river basin *SWAT* (Arnold et al., 1998) and the reduced-complexity *SedNet* (Prosser et al., 2001) models at continuous temporal scale, and also the event-based *TOPMODEL* (Beven et al., 1995) and *EUROSEM* (Morgan et al., 1998) models.

Previous studies demonstrate that large parts of the world are affected by intense processes of soil degradation and about 10 million ha of cropland are lost each year due to soil erosion, thus reducing the soil available for food production (Pimentel, 2006). In Mediterranean cultivated and set-aside soils the magnitude of erosion rates significantly varies throughout the year and seasons due to changes in the soil, climate and plant phenology (e.g. De Santisteban et al., 2006; López-Vicente et al., 2008 and Fiener et al., 2011). Thus, there is a necessity to develop an accurate, adaptable and easy-to-run model to predict spatially distributed values of runoff, soil erosion and redistribution at a monthly scale instead of the commonly used empirical annual-based models or the complex event scale models. In this study we present the Soil Erosion and Redistribution Tool (*SERT*) model and the results of its application in a small Mediterranean agricultural catchment with a detailed database. Run in a GIS environment, the *SERT* model predicts average monthly values of runoff production, soil erosion and sediment redistribution. This model has been developed with the aim of coupling the physically-based equations of the *DR2* (López-Vicente and Navas, 2012) water balance model, with the structure of the *RMMF* (Morgan, 2001) and *Modified MMF* (Morgan and Duzant, 2008) models of soil erosion and sediment delivery, and the conceptual basis of the Index of Connectivity (*IC*) of Borselli et al. (2008) that includes the role of the man-made infrastructures. The *SERT* model has been designed to account for the temporal variations in climatic and vegetation parameters and tillage practices that occur throughout the year. Validation procedure is carried out with rates that are quantified with the radionuclide ^{137}Cs in 133 control points. The topography of the study area is controlled by the presence of a sinkhole and thus is a closed-hydrological system where the balance between the amount of soil loss and deposition can be calculated accurately. The *SERT* model aims to be an accurate, easy-to-run, low-input-demanding management tool of spatially distributed runoff and soil erosion and redistribution for small and medium size agricultural catchments.

2. Material and methods

2.1. The SERT model

The Soil Erosion and Redistribution Tool (*SERT*) model is a semi-physically-based approach to predict monthly rates of runoff depth, soil erosion in rill and interrill areas and sediment redistribution in small and medium size catchments. Processes that take place in permanent water courses (e.g., creeks, rivers, ponds, dams) are not considered and thus the *SERT* model is not suitable for large catchments or river basins. The *SERT* model divides the simulation procedure into four modules: i) hydrology (*SERT-Hy*), ii) soil erosion (*SERT-Er*), iii) soil redistribution (*SERT-Rd*) and iv) modelling validation (*SERT-V*) (Fig. 1). As the *SERT* model is run at monthly scale most of its inputs are measured and calculated at monthly scale (Table 1). The *SERT* model has the conceptual basis and part of the equations of the *DR2*, *RMMF* and *IC* models, to which are added water and sediment balance factors to achieve an accurate prediction ability. The other novel aspect of this model, in comparison with other similar models, is the high number of processes that can be simulated with a moderate number of inputs.

2.1.1. The hydrologic module (SERT-Hy)

The GIS-based water balance Distributed Rainfall-Runoff (*DR2*) model (López-Vicente and Navas, 2012) yields the basis of the hydrological module. The *DR2* model computes the depth of water stored and infiltrated in the soil profile and the runoff depth considering spatial and temporal variations in rainfall intensity, soil saturation and upslope contribution factors. This model was run in the medium size Estaña Lakes catchment, where the small study area of this research is located, and it allowed humidity variations and trends in time and space to be monitored. The *DR2* model calculates the monthly effective cumulative runoff ($CQ_{eff\text{-}m}$, mm) following a three-step procedure. In the first step, the unsaturated cells and cells saturated by direct rainfall (no runoff contribution) are differentiated. Time to ponding, *Tp* (s), is the time it takes for the soil surface to become saturated in conditions of rainfall intensity greater than the saturated hydraulic conductivity of the topsoil (K_{fs}, cm s^{-1}) and is calculated as the mean value between the minimum and maximum time to ponding, following the approach of Hogarth et al. (1991):

$$\frac{1}{2}\frac{Sp_{im}^2}{K_{fs}}\ln\left(\frac{I_m}{I_m - K_{fs}}\right) \le Tp_{im} \le \frac{1}{2}\frac{Sp_{im}^2}{I_m - K_{fs}} \quad (1)$$

$$Sp_{im} = \sqrt{2 \cdot (\Delta\theta_{im})\phi_i} \quad (2)$$

$$\Delta\theta_{im} = \theta_{Seff-i} - \theta_{0-im} \quad (3)$$

where *Sp* is the soil sorptivity (cm s$^{-0.5}$), *I* (cm s^{-1}) is the average rainfall intensity, ϕ is the matrix flux potential (cm^2 s^{-1}) of each soil type, and θ_{Seff} (% vol.) and θ_0 (% vol.) are the effective saturated and initial volumetric water content of the soil, respectively. The subscripts *i* and *m* correspond to each cell of the digitalized study area, and each month of the year, respectively. The initial water content is the volume directly measured in the field (antecedent topsoil moisture), the θ_{Seff} parameter accounts for the maximum amount of water that can be stored within the soil taking into account the volume of rocks and $\Delta\theta$ is the difference between both values. Coarse fragments play a critical role in the processes of topsoil saturation and initiation of runoff (Smets et al., 2011) and are very frequent in the Mediterranean soils and thus have to be considered in studies of soil redistribution (Soto and Navas, 2008). Once topsoil is saturated overland flow appears and the initial runoff per raster cell, Q_0 (mm), is estimated as a function of the depths of effective rainfall, *ER* (mm), rainfall to ponding, *Rp* (mm), and the average number of rainfall events, *e* (n):

$$Q_{0im} = ER_{im} - (Rp_{im}\, e_m) = ER_{im} - (Tp_{im}\, I_m\, e_m) \ge 0 \quad (4)$$

$$ER_{im} = R_m (1 - A_{im}) \cos S_i \quad (5)$$

Values of *ER* are estimated after considering the depth of precipitation intercepted by the canopy of the crops and natural vegetation, *A* (0–1), from the total rainfall depth, *R* (mm), and using the improvement presented by Morgan and Duzant (2008) to consider the effect of slope angle, *S* (radians), on the quantity of rain received per unit area. Once time to ponding and initial runoff are calculated at each sampling point, the corresponding maps for the whole catchment are created with the Kriging interpolation method (ordinary type with constant trend removal) that gets the minimum standard error. In the second step of the DR2 model, initial runoff is routed into the digital elevation model (*DEM*) of the catchment using the multiple flow accumulation algorithm ($Acc.Algorithm_{MD}$), with a coefficient of concentration of 0.9 and the potential cumulative runoff, CQ_0 (mm), is obtained. The subscript *resol* corresponds to the spatial resolution of the *DEM* because the depth of calculated cumulative runoff also depends on this parameter. In the *SERT-Hy* module the effect of the man-made linear landscape elements (*LLEs*) is added as effective players modifying the natural runoff connectivity along the hillslopes and fields. This concept is based on the index of connectivity (*IC*) presented by Borselli et al. (2008) and successfully used by these authors and by others (e.g. Cavalli et al., 2012; López-Vicente et al., 2013) in medium-size agricultural and mountainous catchments in Italy and Spain to identify areas with net soil loss and deposition.

$$CQ_{0m} = f\left(Q_{0im}, \mathrm{Acc.Algorithm}_{\mathrm{MD}}^{c=0.9}, LLEs, \mathrm{DEM}_{\mathrm{resol}}\right) \quad (6)$$

As there are many types of cumulative algorithms, and each type generates a different map with different values, a water balance correction factor (α) is added to achieve that the volume of balanced potential cumulative runoff (CQ_{0B}) equals the initial volume of available water to be accumulated along the catchment. The "α" factor allows other users of the *SERT* model to choose whatever type of cumulative algorithm they wish to use. A map including all *LLEs* was created and a mask with two values, 0 for the *LLEs* and 1 for the remaining area, was created to modify the map of flow direction used in the flow accumulation algorithm. The effective cumulative runoff, CQ_{eff} (mm), is calculated after considering the saturated hydraulic conductivity, K_{fs} (mm s^{-1}), and the average duration of a storm after the soil becomes saturated until the end of the rainfall event for each month *m*, Tq_m (s):

$$CQ_{0Bm} = \alpha \cdot CQ_{0m} = \frac{\sum_{i=1}^{i=k} ER_{im} - \sum_{i=1}^{i=k} Rp_{im}\, e_m}{\sum_{i=1}^{i=k} CQ_{0m}} \cdot CQ_{0m} \quad (7)$$

$$CQ_{eff-m} = \left(CQ_{0Bm} - K_{fs}\, Tq_m\, ee_m - SS_{\max-m}\, ee_m\right) \sin S \quad (8)$$

$$Tq_m = (TER_m - Tp_m) + Tq_{AftER} = (TER_m - Tp_m) + \left(FlL / FlV\right) \quad (9)$$

and the maximum amount of water retained on the soil surface, SS_{max} (mm), according to Driessen (1986):

$$SS_{\max-m} = 0.5\,RG_m \frac{\sin^2(SIG - S)}{\sin(SIG)} \frac{\cot(SIG + S) + \cot(SIG - S)}{2\cos(SIG)\cos(S)} \tag{10}$$

where ee_m (n) is the average number of monthly rainfall erosive events, TER_m (s) is the total duration of an average monthly storm event, *FlL* (m) is the flow length, *FlV* (m/s) is the flow velocity, *RG* (mm) is the surface roughness, i.e. the maximum depth of the soil microrelief, *SIG* (radians) is the surface soil and surface furrow angle, and *S* (radians) is the slope angle of the land. An erosive event has a rainfall amount >12.7 mm or a peak rainfall intensity >6.35 mm in 15 min (Renard et al., 1991). A *SIG* value of 30º is used in the study area according to the value used in the previous application of the *DR2* model. Surface roughness is the configuration of the soil caused by the randomly orientated arrangement of soil clods. In this work the roughness value for forest areas (random roughness, *RG* = 20.3 mm) was taken from Renard et al. (1991). Tillage tools produce random and orientated roughness. For the tillage direction perpendicular to the contours, *RG* is the roughness immediately after tillage and before rainfall, and it is 32 mm for the plough, 23 mm for the heavy cultivator and 18 mm for the disk-harrow (Gilley and Finkner, 1991). For the tillage direction parallel to the contours, *RG* is the orientated surface roughness, which can be considered to be equal to the initial tillage depth immediately after tillage and before rainfall (250 mm for the plough, 150 mm for the heavy cultivator and 80 mm for the disk-harrow).

2.1.2. The soil erosion module (SERT-Er)

The *SERT-Er* module calculates the monthly splash (F_m, Mg ha^{-1} month^{-1}) and runoff (H_m, Mg ha^{-1} month^{-1}) detachment rates according to the revised Morgan, Morgan and Finney (*RMMF*) model (Morgan, 2001) and it compares the sum of these rates with the runoff transport capacity (TC_m, Mg ha^{-1} month^{-1}) to predict the monthly rates of soil erosion (E_m, Mg ha^{-1} month^{-1}):

$$E_m = \min(F_m + H_m, TC_m) \tag{11}$$

$$F_m = K \cdot EE_m \cdot 10^{-2} \tag{12}$$

$$H_m = Z_i \cdot CQ_{eff-m}{}^{1.5} \cdot (1 - GC_m) 10^{-2} \tag{13}$$

$$Z_i = \frac{1}{0.5 \cdot COH_i} \tag{14}$$

$$TC_m = C_m \cdot P \cdot CQ_{eff-m}{}^{\beta} \cdot 10^{-2} \tag{15}$$

where *K* (g J^{-1}) is the soil erodibility, *EE* (J m^{-2}) is the total rainfall energy, *Z* (kPa^{-1}) is the resistance of the soil to being detached and delivered, *GC* (%) is the ground cover (e.g. rocks, litter and stubble), *COH* (kPa) is the cohesion of the soil estimated from the soil texture, and *C* and *P* are the factor of cover management and support practices of the *RUSLE* model (Renard et al., 1991). The β factor range [1.3–2.9] in order to model the loss of transport capacity due to runoff from the divides to the bottom of the hillslope as runoff increase the load of sediment delivered. The map of the β factor was obtained from the map of effective cumulative runoff. In the original *RMMF* model, the runoff depth is not accumulated along the hillslope and it is calculated according to the critical value of soil moisture storage and the mean rain per rainday and total rainfall volume. In the *SERT* model, runoff depth is spatially distributed and computed using the approach described in the hydrological module. Rainfall energy is estimated as the sum of the kinetic energy of the leaf drainage raindrops *E(LD)* (J m^{-2}) and the energy of the direct throughfall rainfall *E(DT)* (J m^{-2}):

$$EE_m = E(DT)_m + E(LD)_m \quad (16)$$

$$E(DT)_m = DT_m \cdot KE_m \quad (17)$$

$$E(LD)_m = (15.8\, PH_m^{0.5}) - 5.87 \quad (18)$$

where DT_m (mm) is the direct throughfall volume of monthly rainfall estimated from the total depth of effective rainfall (ER_m, mm) and the depth of leaf drainage (LD_m, mm), and KE_m (J m^{-2} mm^{-1}) is the kinetic energy of the rain at each month:

$$DT_m = ER_{im} - LD_m \quad (19)$$

$$LD_m = ER_m \cdot CC_m \quad (20)$$

where CC_m (0–1) is the percentage of the soil surface protected by the canopy. Monthly variations in the values of the A_m, see Eq. (5), and CC_m factors are associated with the phenology of the crops and the presence of deciduous trees. The kinetic energy of the rain is a function of the rainfall intensity, *I* (mm h^{-1}), and is estimated in this study using the equation developed by Coutinho and Tomás (1995) and considered suitable for the western Mediterranean areas:

$$KE_m = 35.9\,(1 - 0.559 \exp(-0.034\, I_m)) \quad (21)$$

2.1.3 The soil redistribution module (SERT-Rd)

As described in the *Modified MMF* (Morgan and Duzant, 2008) model, soil redistribution is the result of a balance between the amounts of soil detached by raindrop impact (F_m, Mg ha^{-1} $month^{-1}$) and by runoff (H_m, Mg ha^{-1} $month^{-1}$) and the amount of delivered soil which is deposited downslope. Using this conceptual basis, the *SERT-Rd* module estimates the

Remaining runoff Transport Capacity ($TC_{r\text{-}m}$, Mg ha^{-1} month^{-1}) factor that allows a different relocation of the sediments from one month to another month as a consequence of the significant temporal changes that happen in the number, duration and intensity of the rainfall events, runoff depth, and tillage practices. Thus, the potential ($DEP_{pot\text{-}m}$, Mg ha^{-1} month^{-1}) and net (DEP'_{m}, Mg ha^{-1} month^{-1}) rates of monthly soil deposition in each cell of the modeled study area are calculated. When the runoff transport capacity (TC_m, Mg ha^{-1} month^{-1}) is the limiting factor of soil erosion in a cell, there is not enough energy for the downwards delivery of the sediment coming from the upslope cells ($E_{up\text{-}m}$, Mg ha^{-1} month^{-1}). Conversely, when the total rate of detached particles is lower than the rate of TC_m, there is a remaining runoff Transport Capacity per cell, $TC_{r\text{-}m}$, and accumulated one along the hillslope ($TC_{r\text{-}up}$, Mg ha^{-1} month^{-1}) that can deliver part or the whole amount of sediment coming from the upslope cells:

$$TC_{r-m} = \left(TC_m - E_m\right) > 0 \tag{22}$$

$$E_{up-m} = f\left(E_m, \mathrm{Acc.Algorithm}_{\mathrm{MD}}^{\mathrm{c=1.1}}\right) \forall \, \mathrm{surface}\, TC_{r-m} > 0 \tag{23}$$

$$TC_{r-up-m} = f\left(TC_{r-m}, \mathrm{Acc.Algorithm}_{\mathrm{MD}}^{\mathrm{c=1.1}}\right) \forall \, \mathrm{surface}\, TC_{r-m} > 0 \tag{24}$$

$$DEP'_m = DEP_{pot-m} - E_m = \left(E_{up-m} - TC_{r-up-m}\right) - E_m \; \forall \, \mathrm{surface}\, DEP'_m > 0 \tag{25}$$

We use a multiple flow accumulation algorithm ($Acc.Algorithm_{MD}$) with a concentration coefficient equal to 1.1 to redistribute the detached particles. Although overland flow accumulation, Eq. (6), and sediment redistribution, Eq. (23), happen simultaneously in nature, we divide these processes into two different equations to facilitate the computational process, and also assign two different values for the *c* coefficient of concentration in order to distinguish the spatial redistribution of runoff and detached particles. Finally, the balance between the total rates of soil loss, sediment deposited and sediment yield at the outlet of the catchment should be zero. The presence of karstic processes and the development of a sinkhole at the bottom of the study area prevent the occurrence of the typical outlets associated with rivers and gullies, and thus the balance is performed between rates of soil loss and deposition:

$$DEP_m = DEP'_m \cdot x \tag{26}$$

$$x = \frac{LOSS_{T-m}}{DEP'_{T-m}} \tag{27}$$

where DEP_m (Mg ha^{-1} month^{-1}) is the weighted rate of soil deposition, and x is the weighting factor between the values of total soil loss ($LOSS_{T\text{-}m}$, Mg month^{-1}) and total deposited sediment before weighting ($DEP'_{T\text{-}m}$, Mg month^{-1}). On a yearly basis, values of soil redistribution are computed as the sum of the processes of soil redistribution that happen in each month of the year:

$$RED_{yr} = \sum_{m=1}^{m=12} DEP_m - \sum_{m=1}^{m=12} LOSS_m \qquad (28)$$

2.1.4 Model analysis and validation with ^{137}Cs derived rates

A sensitivity analysis was carried out to test that the model behaved rationally and to determine which input parameters had most effect on the predictions of runoff and soil erosion. Sensitivity was analysed using the average linear sensitivity (*ALS*) approach (McCuen and Snyder, 1986), which expresses a relative normalized change in output to a normalized change in input:

$$ALS = \frac{\left[O_2 - O_1 \middle/ \bar{O}_{1,2} \right]}{\left[I_2 - I_1 \middle/ \bar{I}_{1,2} \right]} \qquad (29)$$

where O_1 and O_2 are the values of the model output obtained with the values of I_1 and I_2 for input parameter *I*, and $\bar{I}_{1,2}$ and $\bar{O}_{1,2}$ are the means of the two input and two output values respectively. This approach is appropriate for comparing the sensitivities of input parameters with values of different orders of magnitude and has been used to perform sensitivity analysis in other erosion predicting models such as *WEPP* (Nearing et al., 1990) and *Modified MMF* (Morgan and Duzant, 2008). Although it does not deal well with sensitivity when the output of the model is related non-linearly to an input, this issue can be addressed by examining how the value of *ALS* changes as the input is varied over small ranges.

The validation process of the predicted soil redistribution rates constitutes the *SERT-V* module and is adaptable to any method that can provide accurate values of net soil loss and deposition along the catchment or sediment yield at the outlet. In this study we use spatially distributed rates of soil loss and deposition quantified with ^{137}Cs. Caesium-137 derived from nuclear testing in the past century has been widely used as a sediment tracer of soil redistribution, providing information on medium term (40–50 years) erosion rates. As the *SERT* model has been run with average weather data for a period of fifteen years, not at event or specific year scale, output maps and rates were also average predictions and thus the choice of the aforementioned radionuclide technique seems to be very adequate for our study. Additionally, the study area did not have a river or a creek where a gauging station could be installed to measure sediment delivery. In this study we use the models of Soto and Navas (2004, 2008) to quantify the net rates of soil redistribution. In order to ensure the reliability of the Cs-137 technique to provide accurate values of soil redistribution any soil sample with a high content of organic matter and/or coarse fragments was removed. The ^{137}Cs activities were measured using a high resolution, low background, coaxial gamma-ray detector of hyperpure germanium coupled to an amplifier and multichannel analyser. The efficiency of the detector is 30%, with 1.92 keV resolution (shielded to reduce background) and was calibrated using certified standard samples of the same geometry as the measured samples. Gamma emissions of ^{137}Cs (662 keV line in mBq g^{-1} air-dry soil) were measured for the soil samples with a counting time of 30,000 s (more details about the method in Navas et al., 2012).

2.2. Study area and field survey

The study area is a small sub-catchment, the so-called *Pilot catchment*, of the Estaña Lakes catchment which is located in the Spanish Pyrenean Marginal Ranges and within the Ebro River Basin (Fig. 2a). The land uses and the physiographic characteristics of this agro-ecosystem are those typically found in the Mediterranean rain-fed agricultural systems. The study area has a reduced area of 0.73 ha, elevation ranges between 686 and 698 m a.s.l. and the mean slope steepness is 17%. Steep slopes (*S* higher than 22.5%) occupy 28% of the study area and are associated with the walls of the sinkhole that appears in the *Pilot catchment* whereas gentle slopes are cultivated with winter cereals (wheat and barley) (*S* lower than 8%) and cover 18%. This area has a relatively long history (dating back to the 10th century) of human occupation, agricultural practices and water management (Morellón et al., 2011). Natural and anthropogenic areas are heterogeneously distributed in small patches and numerous stone-walls appear in the study area modifying the natural dynamics of runoff and sediment connectivity (López-Vicente et al., 2013). The *Pilot catchment* has two fields of winter cereal that cover 30% of the study area, and a dense Mediterranean forest of dry-resistant deciduous oaks (*Q. faginea*) and holm oaks (*Quercus rotundifolia* and *Q. coccifera*) that occupy another 53%. Patches of Mediterranean shrubs (mainly *Buxus sempervirens*, *Juniperus oxycedrus* and *Rosmarinus officinalis*) and meadows cover 13% of the study area (Fig. 2b, c). The other 4% is associated with a small settlement, a man-made accumulation of rocks and the unpaved trail that connect the cultivated areas with the rest of the Estaña Lakes catchment.

Climate is continental Mediterranean with two humid periods, one in spring (April and May) and a second in autumn (September and October). Low summer precipitation causes summer droughts and long periods of low rainfall depth trigger severe damage in natural vegetation and crops. At Canelles weather station, located 8 km to the southeast of the study area, the mean annual precipitation for the reference period 1961-1990 considered by the World Meteorological Organization, was 520 mm whilst over the last fifteen years (1997-2011) it was 13% lower (454 mm) (data source: Ebro Basin Water Authorities). Annual precipitation has a strong inter-annual oscillation that for the period 1941–2011 was 378%. From an average number of 83 annual rainfall events only 11 had a precipitation above 12.7 mm and could be considered as erosive events following the definition proposed by Renard et al. (1991). The average maximum rainfall intensity in 30 min, I_{30}, is higher than 16 mm h^{-1} between May and October with highest values in August and September (ca. 25 mm h^{-1}) and below 7 mm h^{-1} in winter months (Fig. 2d, e). All weather inputs were obtained from the values recorded every 15 minutes at Canelles weather station over a period of fifteen years (1997-2011).

The Estaña Lakes catchment has a complex geological and geomorphological history (see López-Vicente et al., 2009 and Pérez-Bielsa et al., 2012) that explains the variety of the parent material of the soils: Mesozoic gypsiferous marls, dolomites, limestones and Holocene doline deposits. Six types of soils are distinguished using the FAO classification (Machín et al., 2008) that can be grouped into three main types: Calcisols (covering 60% of the total surface area, which is mainly cultivated), Leptosols (39% and covered with forest) and Regosols (1%) (Fig. 2f). Texture is mainly silty loam and in some parts sandy loam, loam and silty clay. A total number of 266 soil samples were collected using a regular 5x5 metre grid (Fig. 2g) in spring 2007. Samples were air-dried, ground, homogenized and quartered to pass through a 2 mm sieve. The different inputs related to the soil properties were measured and calculated using the soil samples and direct measurements in the field (more details in López-Vicente, 2008).

Large areas of this study site are affected by active soil erosion by water, as described in the literature (e.g. Soto and Navas, 2008; López-Vicente and Navas, 2009; Gaspar et al., 2013) with high rates of soil loss mainly having an impact on crops (ranging from almost zero to 108 Mg / ha yr) and areas with low vegetation cover (unpaved trails, disperse scrublands) and those located on steep slopes. However, the magnitude of the erosion process varies significantly throughout the year and thus monthly values of soil erodibility and net soil loss also vary (López-Vicente et al., 2008). Active processes of sediment delivery and soil redistribution along the hillslopes and the influence of man-made linear landscape elements (LLEs) on the processes of runoff accumulation and sediment trapping effectiveness have been also described in detail in this study area (López-Vicente et al., 2013; Navas et al., 2012). To assess the accuracy of the soil loss and deposition predictions with *SERT* and to perform the validation procedure, 133 control points (*CPs*) were established along the whole *Pilot catchment*. The *CPs* were located every two soil sampling sites using a regular 10x10 metre grid to obtain 45 *CPs* for the cultivated area, 60 for the oak forest, 10 for the holm oak forest, 5 for the scrublands, 9 for the pastures and 4 for the unpaved trails and areas of bare soil. The extensive database available and the background of prior studies performed in the *Pilot catchment* provide an excellent frame to run and test the new *SERT* model in this location.

3. Results and discussion

3.1. Runoff and Soil erosion

The initial runoff depth generated per raster cell, Q_0, reveals significant variations in time and space. As can be seen in Figure 3a, mirroring the spatial distribution of the different soil types, those areas with higher values of saturated hydraulic conductivity present the lowest values of annual runoff depth. This spatial trend remains constant throughout the twelve months of the year although the differences in the monthly values become more significant in the six month period from November to April, when the intensity of rainfall events decreases significantly. Runoff coefficients related to the values of Q_0 are plotted in Figure 3b and show that no runoff is expected in Haplic Calcisols (*CLha*) for six months and in Rendzic Leptosols (*LPrz*) for five months. The average annual runoff coefficient decreases from 99.6% in Leptic Calcisols (*CLle*) to 97.8% in Haplic Calcisol with Haplic Leptosol (*CLha* + *LPha*) 57.8% in *LPrz* and 44.1% in *CLha*. These results highlight the key role played by the factors associated with the different soil types, especially the saturated hydraulic conductivity of the topsoil, K_{fs}, see Eq. (1), to explain the temporal and spatial variability of time to ponding, initiation of runoff and total runoff depth. As for the average volume of water stored on the soil surface, SS_{max-m} in Eq.(8), this varies between 4 and 7 mm due to the different tillage practices throughout the year. The *ALS* of the *SERT-Hy* module, see Eq. (29), was performed on the values of effective cumulative runoff (CQ_{eff}) in October when the maximum values of overland flow occur, showing that sensitivity is greatest for the factors of upslope contributing area (*ALS* = 1.38), slope steepness (*ALS* = 0.86), soil roughness (*ALS* = 0.42) and saturated hydraulic conductivity (*ALS* = 0.37), and to a lesser extent, for the matrix flux potential (*ALS* = 0.11). The *ALS* of CQ_{eff} for the other inputs is low (*ALS* < 0). In addition, in relation to the two most important factors, values of CQ_{eff} present high sensitivity in the ranges of low upslope contributing areas and high slope steepness.

The *SERT-Er* module predicted an average annual erosion rate of 11.04 Mg ha^{-1} yr^{-1} for the whole *Pilot catchment* (Fig. 4a). This value clearly exceeds the maximum tolerable rate of 1.4 Mg ha^{-1} yr^{-1} proposed by Verheijen et al. (2009) for the prevalent conditions in European cultivated lands and hence poses a threat to the sustainability of this agro-ecosystem. The above-described spatial pattern of soil erosion remains almost constant throughout the year although average values vary significantly between low average erosion rates in January, February and July (below 0.15 Mg ha^{-1} month^{-1}) and the higher values in April, May, September, October and November (between 0.8 and 1.9 Mg ha^{-1} month^{-1}) (Fig. 4b). Monthly rainfall depths correlate well with monthly average and standard deviation (*sd*) values of soil erosion in the whole catchment (Pearson's r = 0.96 and 0.85, respectively), whereas rainfall intensity correlates poorly with the average (r = 0.25) and the *sd* values (r = 0.27) of soil erosion. The same temporal pattern is observed in the percentages of eroded and non-eroded areas (Table 2). Soil erosion is mainly triggered in five months (April, May, September, October and November) totalling 86, 86, 84 and 80% of the total annual erosion in *CLha*, *CLha* + *LPha*, *CLle* and *LPrz*, respectively. The highest rates always occur in October but the temporal pattern of the values of soil erosion change in the case of different soil types (see bold numbers in Table 2). Additionally, no linear relationship has been found between the percentage of eroded area and the mean values of soil erosion, indicating the complexity of the processes of soil detachment and delivery. The percentage of soil surface affected by water erosion is very high and almost constant between April and October in the four soil types, whereas the largest areas without soil erosion are predicted in winter, with the largest surface without soil erosion occurring in March. The temporal patterns of runoff depth and soil erosion described with *SERT* mainly agree with those highlighted by López-Vicente et al. (2008) in cultivated lands of the Estaña Lakes catchment and by other authors in similar landscapes and climatic conditions (e.g. Renschler et al., 1999) although the *SERT* model emphasizes the monthly differences in the magnitude and extension of the soil affected by water erosion. This characteristic of the *SERT* model makes it more valuable to obtain a detailed assessment of the risk of soil erosion in each month and erosion period of the year.

Cultivated (*CLha* and *CLha* + *LPha*) and bare (*CLha* + *LPha*) soils are affected by intense processes of soil erosion and present average rates of 20 and 10 Mg ha^{-1} yr^{-1}, respectively. High values of soil erosion also affect the soils of the Mediterranean forest and oak forest (9.1

and 8.2 Mg ha^{-1} yr^{-1} on average, respectively) due to their location on steep slopes while pastures and scrublands display the lowest soil erosion values, with average rates of 1.7 and 2.3 Mg ha^{-1} yr^{-1}, respectively. Predicted rates of soil erosion in the cropland of the *Pilot catchment* are in the same range of magnitude as those estimated with ^{137}Cs by Gaspar et al. (2013) and Navas et al. (2012) and with the *RMMF* model by López-Vicente and Navas (2010) in other cultivated soils in the Estaña Lakes catchment. The highest values appear in those areas where cumulative runoff and slope steepness reach high values and soil surface is bare during some months or throughout the whole year. We consider that further research should be done to improve the runoff connectivity estimation along the walls of the sinkhole where many blocks of limestone appear as well as cloggy soils (López-Vicente et al., 2009). In addition, it seems necessary to account for the processes of percolation as the study area presents karst processes that have not been considered in the estimation of the cumulative runoff depth. On a monthly basis and selecting the month of October which is when the highest values of soil erosion occur, the average linear sensitivity (*ALS*) of the predicted rates of soil erosion is greatest for the inputs of slope steepness (*ALS* = 4.62), effective cumulative runoff (*ALS* = 3.23) and the *C-RUSLE* factor (*ALS* = 1.19) and, in a minor way, for the soil cohesion (*ALS* = 0.56) and soil detachability (*ALS* = 0.25) factors. On the other hand, the *ALS* of the rates of soil erosion is below zero for plant height, canopy cover, rainfall interception and surface cover factors.

3.2. Soil Redistribution and modelling validation

Soil redistribution was estimated for each month of the year, revealing significant variations in the values and areas affected by soil loss and deposition (Fig. 5). The temporal variations in the magnitude of the values mirror the variability described in the monthly rates of soil erosion, although the spatial changes reflect the temporal and spatial variability in the rates of splash (F_m) and runoff (H_m) detachment, transport capacity (TC_m), and remaining transport capacity ($TC_{r\text{-}m}$). Stable areas, without processes of soil loss or deposition, are relatively frequent in January (2.6% of the total surface), February (1.3%), March (2.6%), July (1.3%), November (2.1%) and December (2.2%), whereas for the other six months the percentage remains ca. or below 1%. Predominantly, soil loss processes take place in February, June, July and August when the percentage of the soil surface affected by net soil loss is above 85%, whereas soil deposition affects larger areas in March, April, May, September, October and December (between 28 and 51% of the soil surface). There is a positive correlation between the intensity of soil erosion processes and the surface of the bottom of the catchment affected by sediment deposition (Pearson's r = 0.825). These results show the complexity of the processes of soil loss and sediment delivery and deposition and contribute valuable information to previous studies relating to seasonal dynamics of runoff-contributing areas (Latron and Gallart, 2007) and sediment delivery (Navas et al., 2009) in the Spanish Pyrenees and other agricultural landscapes (e.g. Francia Martínez et al., 2006 in olive orchards).

On an average annual scale, the total surface of the *Pilot catchment* affected by soil loss is 62% and has an average value of soil loss of 10 Mg ha^{-1} yr^{-1}, whereas the remaining surface presents a mean value of soil deposition of 9 Mg ha^{-1} yr^{-1} (Figure 6a). The abrupt changes between values of soil loss and deposition that occur in some parts of the study area can be explained by the effect of the landscape linear elements that interrupt sediment connectivity and by the changes in land uses. The performance of the model is satisfactory and provides statistically significant correlations for total soil redistribution (Pearson's r = 0.709) and soil loss (Pearson's r = 0.652). Predicted values of soil deposition have a lower however satisfactory correlation with quantified values with ^{137}Cs (Pearson's r = 0.564) (see Figure 6b). Considering each sampling point as a test point, the Nash-Sutcliffe coefficient was 0.48, showing the good prediction ability of the *SERT* model and also highlighting the high quality of the modelling parameterization carried out in this study. The performance values have to be evaluated taking into account that the analytical precision of the measurements done with ^{137}Cs is approximately ±5% and the processes of soil loss and deposition are modelled separately with the ^{137}Cs measurements.

The analysis of soil redistribution for the different land uses was performed with both observed (^{137}Cs) and predicted (*SERT-Rd*) values (see Table 3). Cultivated areas present high rates of both soil loss and deposition which, on average, range between -11 and 13 Mg ha^{-1} yr^{-1}. The standard deviation values are also high. Conversely, mean rates of soil loss and deposition in rangeland are much lower and high rates only appear on small patches. These values reveal the heterogeneity of the processes of soil redistribution in the *Pilot catchment*. Finally, the sediment balance predicted with the *SERT-Rd* model was -1.15 Mg yr^{-1} and the observed balance of soil redistribution with ^{137}Cs was -0.59 Mg yr^{-1}. Both values are similar, negative and close to zero and can be considered to be a good estimation since the *Pilot catchment* is an endorheic area affected by moderate karst processes. As the topographic characteristics of the study area enable the accurate estimation of the sediment balance, the predictions of the *SERT* model should be improved in further research, considering the processes of percolation of fine particles on the lowlands where the sinkhole is slightly active, the deposition of soil particles in the cloggy soils, and the occurrence of tillage erosion. In order to broaden the use of the *SERT* model in other study areas, further research will also focus on developing a calibration module using the β factor, Eq. (15), for monitored catchments where data of sediment delivered in gullies and river systems are available.

4. Conclusions

The *SERT* model has proved to be an accurate model for small and medium-size catchments to estimate monthly and annual rates of runoff depth, soil erosion and sediment redistribution, taking advantage of current GIS-based techniques. The ability of the new model to discriminate stable areas and the high sensitivity of the model to predict different spatial and temporal patterns of initial runoff, total runoff depth, and soil loss and deposition makes the *SERT* model a useful tool for soil and hydrologic simulations. With a total number of 24 input parameters, the *SERT* model requires a significantly lower number of inputs than other spatially distributed and temporal continuous models, and thus the new approach can be easily run for studies of soil erosion risk, especially in areas with limited information. In addition, the four-module structure of the *SERT* model makes it adaptable to any method that can provide accurate rates of cumulative runoff and net soil loss and deposition throughout the catchment or at the outlet. After validation with ^{137}Cs derived rates the performance and good parameterization of the *SERT* model has been successfully proved. Finally, the application of the new model in the *Pilot catchment* has provided valuable information on the processes of soil saturation, runoff and soil redistribution that can be used in other agro-ecosystems. In order to extend the use of the *SERT* model we are currently developing a module for open-source and free *SAGA* GIS software that will be called *SERT-2013 SAGA v1.0*. This module is built using C++ code and contains all scientific methods and equations, and is presented in a user-friendly interface that will be of interest to the scientific and academic community. The module will be available at our research centre website in autumn 2013.

Acknowledgements

This research was funded by the Projects "Erosion and redistribution of soils and nutrients in Mediterranean agroecosystems: radioisotopic tracers of sources and sinks and modelling of scenarios (EROMED) (CGL2011-25486/BTE)" of the Spanish Ministry of Economy and Competitiveness (former Ministry of Science and Innovation) and "Mitigation of siltation of the Estaña Lakes Wetlands (Huesca, Spain) under different scenarios of climate change: soil and water trapping effectiveness of the "green areas" of the new CAP (Expedient number 2012 GA LC 034)" of the Regional Government of Aragón (Spain) and *Obra Social "la Caixa"*.

References

Adams, R., Western, A.W., Seed, A.W., 2012. An analysis of the impact of spatial variability in rainfall on runoff and sediment predictions from a distributed model. *Hydrol Process* **26**(21), 3263–3280

Andrews, R. G., 1954. *The use of relative infiltration indices in computing runoff*, in: Rainfall-runoff relationship (V.P. Singh, Ed.). Water Resources Publications, Littleton, Colo.

Arnold, J.G., Srinivasan, R., Muttiah, R.S., Williams, J.R., 1998. Large Area Hydrologic Modeling and Assessment—Part 1: Model Development. *J Am Water Resour As* **34**(1), 73–89

Beven, K.J., Lamb, R., Quinn, P., Romanovicz, R., Freer, J., 1995. *TOPMODEL*. In: Computer models of watershed hydrology, Signh VP (ed). Water Resources Publications: Highlands Ranch; 627–668

Borselli, L., Cassi, P., Torri, D., 2008. Prolegomena to sediment and flow connectivity in the landscape: A GIS and field numerical assessment. *Catena* **75**(3), 268–277

Cavalli, M., Trevisani, S., Comiti, F., Marchi, L., 2012. Geomorphometric assessment of spatial sediment connectivity in small Alpine catchments. *Geomorphology*, **doi**: 10.1016/j.geomorph.2012.05.007

Cerdà, A., Brazier, R., Nearing, M., de Vente, J., 2013. Scales and erosion. *Catena* **102**, 1–2

Cerdan, O., Couturier, A., Le Bissonnais, Y., Lecomte, V., Souchère, V., 2002. Incorporating soil surface crusting processes in an expert-based runoff model: Sealing and Transfer by Runoff and Erosion related to Agricultural Management. *Catena* **46**(2-3), 189–205

Coutinho, M.A., Tomás, P.P., 1995. Characterization of raindrop size distributions at the Vale Formoso Experimental Erosion Center. *Catena* **25**(1–4), 187–197

De Baets, S., Poesen, J., Meersmans, J., Serlet, L., 2011. Cover crops and their erosion-reducing effects during concentrated flow erosion. *Catena* **85**(3), 237–244

De Roo, A.P.J., Wesseling, C.G., Jetten, V., Ritsema, C.J., 1995. *LISEM: Limburg Soil Erosion Model*. A User Guide, Version 3.1. Department of Physical Geography, Utrecht University, Utrecht, the Netherlands.

De Santisteban, L.M., Casalí, J., López, J.J., 2006. Assessing soil erosion rates in cultivated areas of Navarre (Spain). *Earth Surf Proc Land* **31**, 487–506

Diao, X., Sarpong, D.B., 2011. Poverty implications of agricultural land degradation in Ghana: An economy-wide, multimarket model assessment. *Afr Dev Rev* **23**(3), 263–275

Driessen, P.M., 1986. *The water balance of soil*. In: van Keulen, H., Wolf, J. (Eds.), Modeling of Agricultural Production: Weather, Soils and Crops. Pudoc, Wageningen, The Netherlands, pp. 76–116

Fiener, P., Auerswald, K., Van Oost, K., 2011. Spatio-temporal patterns in land use and management affecting surface runoff response of agricultural catchments-A review. *Earth-Sci Rev* **106**(1-2), 92–104

Foster, G.R., Yoder, D.C., McCool, D.K., Weesies, G.A., Toy, T.J., Wagner, L.E., 2000. *Improvements in Science in RUSLE2*. In: 2000 ASAE Annual International Meeting, Technical Papers: Engineering Solutions for a New Century 2, pp. 2871–2889

Francés, F., Vélez, J.I., Vélez, J.J., 2007. Split-parameter structure for the automatic calibration of distributed hydrological models. *J Hydrol* **332**(1-2), 226– 240

Francia Martínez, J.R., Durán Zuazo, V.H., Martínez Raya, A., 2006. Environmental impact from mountainous olive orchards under different soil-management systems (SE Spain). *Sci Total Environ* **358**(1-3), 46–60

García-Ruiz, J.M., 2010. The effects of land uses on soil erosion in Spain: A review. *Catena* **81**(1), 1–11

Gaspar, L., Navas, A., Walling, D.E., Machín, J., Gómez-Arozamena, J., 2013. Using ^{137}Cs and $^{210}Pb_{ex}$ to assess soil redistribution on slopes at different temporal scales. *Catena* **102**, 46–54

Gilley, J.E., Finkner, S.C., 1991. Hydraulic Roughness Coefficients as Affected by Random Roughness. *T ASAE* **34**(3), 897–903

Gonzalez-Hidalgo, J.C., Batalla, R.J., Cerdá, A., de Luis, M., 2010. Contribution of the largest events to suspended sediment transport across the USA. *Land Degrad Dev* **21**(2), 83–91

Hogarth, W.L., Sardana, V., Watson, K.K., Sander, G.C., Parlange, J.Y., Haverkamp, R., 1991. Testing of approximate expression for soil water status at the surface during infiltration. *Water Resour Res* **27**(8), 1957–1961

Kinsel, W.G. (Ed.), 1980. *CREAMS: A Field Scale Model for Chemicals, Runoff, and Erosion From Agricultural Management Systems*. U.S. Department of Agriculture, Conservation Report No. 26, 640 pp.

Latron, J., Gallart, F., 2007. Seasonal dynamics of runoff-contributing areas in a small Mediterranean research catchment (Vallcebre, Eastern Pyrenees). *J Hydrol* **335**(1-2), 194–206

López-Vicente, M., 2008. *Erosión y redistribución del suelo en agroecosistemas mediterráneos: Modelización predictiva mediante SIG y validación con 137Cs (Cuenca de Estaña, Pirineo Central)*. Doctoral Thesis. University of Zaragoza, Spain. 212 pp.

López-Vicente, M., Navas, A., 2009. Predicting Soil Erosion With RUSLE in Mediterranean Agricultural Systems at Catchment Scale. *Soil Sci* **174**(5), 272–282

López-Vicente, M., Navas, A., 2010. Routing runoff and soil particles in a distributed model with GIS: implications for soil protection in mountain agricultural landscapes. *Land Degrad Dev* **21**(2), 100–109

López-Vicente, M., Navas, A., 2012. A new Distributed Rainfall-Runoff model (DR2) based on soil saturation and runoff cumulative processes. *Agr Water Manage* **104**, 128–141

López-Vicente, M., Navas, A., Machín, J., 2008. Identifying erosive periods by using RUSLE factors in mountain fields of the Central Spanish Pyrenees. *Hydrol Earth Syst Sc* **12**(2), 523–535

López-Vicente, M., Navas, A., Machín, J., 2009. Geomorphic mapping in endorheic catchments in the Spanish Pyrenees: An integrated GIS analysis of karstic features. *Geomorphology* **111**(1-2), 38–47

López-Vicente, M., Poesen, J., Navas, A., Gaspar, L., 2013. Predicting runoff and sediment connectivity and soil erosion by water for different land use scenarios in the Spanish Pre-Pyrenees. *Catena* **102**, 62–73

Machín, J., López-Vicente, M., Navas, A., 2008. Cartografía digital de suelos de la Cuenca de Estaña (Prepirineo Central). In: Benavente, J., Gracia, F.J. (Eds.), Trabajos de Geomorfología en España, 2006-2008. SEG, Cádiz, Spain. pp. 481–484

McCuen, R.H., Snyder, W.M., 1986. *Hydrologic Modeling: Statistical Methods and Applications*. Englewood Cliffs, N.J.: Prentice Hall

Mockus, V., 1949. *Estimation of total (peak rates of) surface runoff for individual storms*, Exhibit A of Appendix B, Interim Survey Rep. Grand (Neosho) River Watershed, USDA, Washington, D.C.

Morellón, M., Valero-Garcés, B., González-Sampériz, P., Vegas-Vilarrúbia, T., Rubio, E., Rieradevall, M., Delgado-Huertas, A., Mata, P., Romero, O., Engstrom, D.R., López-Vicente, M., Navas, A., Soto, J., 2011. Climate changes and human activities recorded in the sediments of Lake Estanya (NE Spain) during the Medieval Warm Period and Little Ice Age. *J Paleolimnol* **46**(3), 423–452

Morgan, R.P.C., 2001. A simple approach to soil loss prediction: a revised Morgan–Morgan–Finney model. *Catena* **44**(4), 305–322

Morgan, R.P.C., Duzant, J.H., 2008. Modified MMF (Morgan-Morgan-Finney) model for evaluating effects of crops and vegetation cover on soil erosion. *Earth Surf Proc Land* **33**(1), 90–106

Morgan, R.P.C., Quinton, J.N., Smith, R.E., Govers, G., Poesen, J.W.A., Auerswald, K., Chisci, G., Torri, D., Styczen, M.E., 1998.The European soil erosion model (EUROSEM): a dynamic approach for predicting sediment transport from fields and small catchments. *Earth Surf Proc Land* **23**(6), 527–544

Navas, A., López-Vicente, M., Gaspar, L., Machín, J., 2012. Assessing soil redistribution in a complex karst catchment using fallout ^{137}Cs and GIS. *Geomorphology*, **doi**:10.1016/j.geomorph.2012.03.018

Navas, A., Valero-Garcés, B., Gaspar, L., Machín, J., 2009. Reconstructing the history of sediment accumulation in the Yesa reservoir: An approach for management of mountain reservoirs. *Lake Reserv Manage* **25**(1), 15–27

Nearing, M.A., Deer-Ascough, L., Laflen, J.M., 1990. Sensitivity analysis of the WEPP hillslope profile erosion model. *T ASAE* **33**(3), 839–849

Pérez-Bielsa, C., Lambán, L.J., Plata, J.L., Rubio, F.M., Soto, R., 2012. Characterization of a karstic aquifer using magnetic resonance sounding and electrical resistivity tomography: a casa-study of Estaña Lakes (northern Spain). *Hydrogeol J* **20**(6), 1045–1059

Pimentel, D., 2000. Soil erosion and the threat to food security and the environment. *Ecosyst Health* **6**(4), 221–226

Pimentel, D., 2006. Soil erosion: a food and environmental threat. *Env Dev Sustain* **8**, 119–137

Pimentel, D., Skidmore, E.L., Trimble, S.W., 1999. Rates of soil erosion (multiple letters). *Science* **286**(5444), 1477–1478

Prosser, I.P., Rutherfurd, I.D., Olley, J.M., Young, W.J., Wallbrink, P.J., Moran, C.J., 2001. Large-scale patterns of erosion and sediment transport in river networks, with examples from Australia. *Mar Freshwater Res* **52**(1), 81–99

Renard, K.G., Foster, G.R., Weesies, G.A., Porter, J.P., 1991. RUSLE – Revised universal soil loss equation. *J Soil Water Conserv* **46**(1), 30–33

Renschler, C.S., Mannaerts, C., Diekkrüger, B., 1999. Evaluating spatial and temporal variability in soil erosion risk—rainfall erosivity and soil loss ratios in Andalusia, Spain. *Catena* **34**(3-4), 209–225

Rivera, S., Ferreira, O.I., de Anguita, P.M., Espinal, F.M., 2011. Soil and economic loss evaluation on small hillside farms in the central mountains of Honduras. *J Sustain Forest* **30**(1), 57-78

Smets, T., López-Vicente, M., Poesen, J., 2011. Impact of subsurface rock fragments on runoff and interrill soil loss from cultivated soils. *Earth Surf Proc Land* **36**(14), 1929–1937

Stavi, I., Lal, R., 2011. Variability of soil physical quality in uneroded, eroded, and depositional cropland sites. *Geomorphology* **125**(1), 85–91

Soil Conservation Service, USDA, 1985. *Hydrology*, National engineering handbook, Supplement A, Sect. 4, Chapter 10. USDA, Washington, D.C.

Soto, J., Navas, A., 2004. A model of ^{137}Cs activity profile for soil erosion studies in uncultivated soils of Mediterranean environments, *J Arid Environ* **59**, 719–730

Soto, J., Navas, A., 2008. A simple model of Cs-137 profile to estimate soil redistribution in cultivated stony soils. *Radiat Meas* **43**(7), 1285–1293

Van Rompaey, A., Verstraeten, G., Van Oost, K., Govers, G., Poesen, J., 2001. Modelling mean annual sediment yield using a distributed approach. *Earth Surf Proc Land* **26**(11), 1221–1236

Verheijen, F.G.A., Jones, R.J.A., Rickson, R.J., Smith, C.J., 2009. Tolerable versus actual soil erosion rates in Europe. *Earth-Sci Rev* **94**(1-4), 23–38

Wischmeier, W.H., Smith, D.D., 1958. Rainfall energy and its relationship to soil loss. *T AGU* **39**, 285–291

Wischmeier, W.H., Smith, D.D., 1978. *Predicting rainfall erosion losses*. Handbook #537. US Department of Agriculture, Washington, DC.

Young, R.A., Onstad, C.A., Bosch, D.D., Anderson, W.P., 1987. *AGNPS, Agricultural Nonpoint-Source Pollution Model: A Watershed Analysis Tool*. U.S. Department of Agriculture, Washington, DC

Figure 1 Flowchart of the *SERT* model. White shapes are based on the *RMMF* model (Morgan, 2001) and grey shapes are specific of the *SERT* model. *SERT-Hy*: Hydrologic module; *SERT-Er*: Soil erosion module; *SERT-Rd*: Soil redistribution module. *V*: Vegetation; *W*: Weather; *T*: Topography; *S*: Soil; *LU*: Land use.

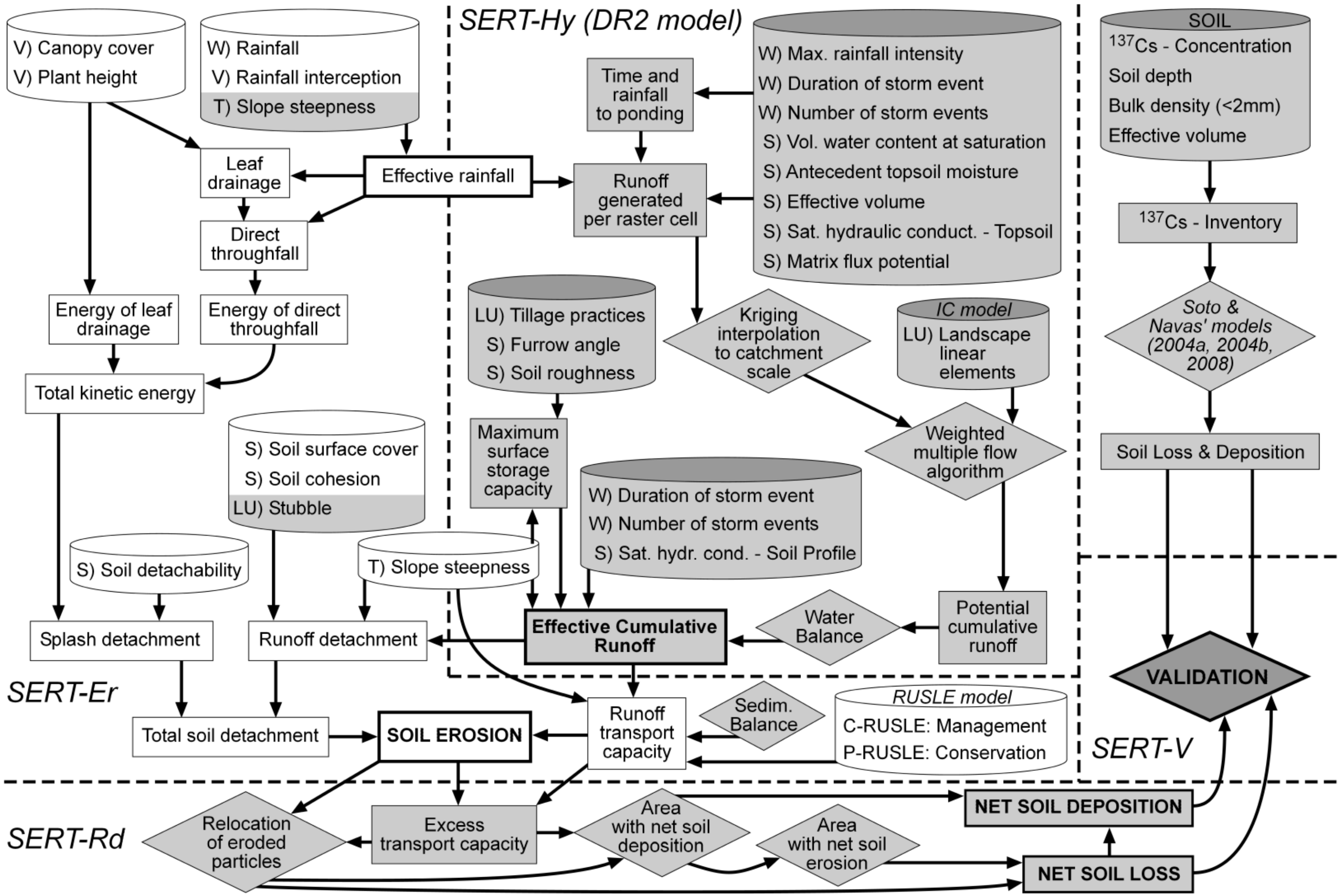

Table 1 Input parameters of the *SERT* model and their temporal variability.

Type of data	Input	Description	Monthly variation
Climatic	R_m	Rainfall depth (mm)	Yes
	I_m	Maximum rainfall intensity (cm s^{-1})	Yes
	TR_m	Average duration of a storm event (s)	Yes
	e_m	Number of erosive rainfall events (n)	Yes
Soil	θ_{Seff}	Effective volumetric water content at saturation (% vol.)	No
	θ_{0m}	Volumetric water content at field conditions (% vol.)	Yes
	Vol_{eff}	Effective volume of the soil (%)	No
	K_{fs}	Saturated hydraulic conductivity (cm s^{-1})	No
	Φ	Matrix flux potential (cm^2 s^{-1})	No
	SIG	Surface soil and surface furrow angle (radian)	No
	RG_m	Soil surface roughness (mm)	Yes
	K	Soil detachability index (g J^{-1})	No
	GC_m	Ground cover, e.g. rocks, litter, stubble (%)	Yes
	COH	Soil cohesion (kPa)	No
	BD_f	Bulk density of fine fraction (<2 mm) (Mg m^{-3}) – only used in the ^{137}Cs model	No
Topography	S	Slope steepness (radian)	No
	MD	Multiple flow accumulation algorithm	No
Land use	LLE	Landscape linear elements (mask)	No
	Tll-Prc	Tillage practices (mask)	Yes
	C	Crop management factor of the RUSLE model (0 – 1)	Yes
	P	Support practices factor of the RUSLE model (0 – 1)	No
Vegetation	A_m	Rainfall interception by canopy (%)	Yes
	CC_m	Canopy cover (%)	Yes
	PH_m	Plant height (m)	Yes

Figure 2 Location of the study area in NE Spain within the Ebro River Basin (a), map of land uses (b), photo of the cereal crop and oak forest (e) monthly values of rainfall and evapotranspiration depth and temperature (d), monthly values of rainfall intensity and number of erosive events (e), map of the different soil types with the location of the soil sampling points (f) and photo of the soil sampling survey (g). *CLha*: Haplic Calcisol; *CLha + LPha*: Haplic Calcisol + Haplic Leptosol; *CLle*: Leptic Calcisol; *LPli + RGli*: Lithic Leptosol + Lithic Regosol; *LPrz*: Rendzic Leptosol; *RGli*: Lithic Regosol.

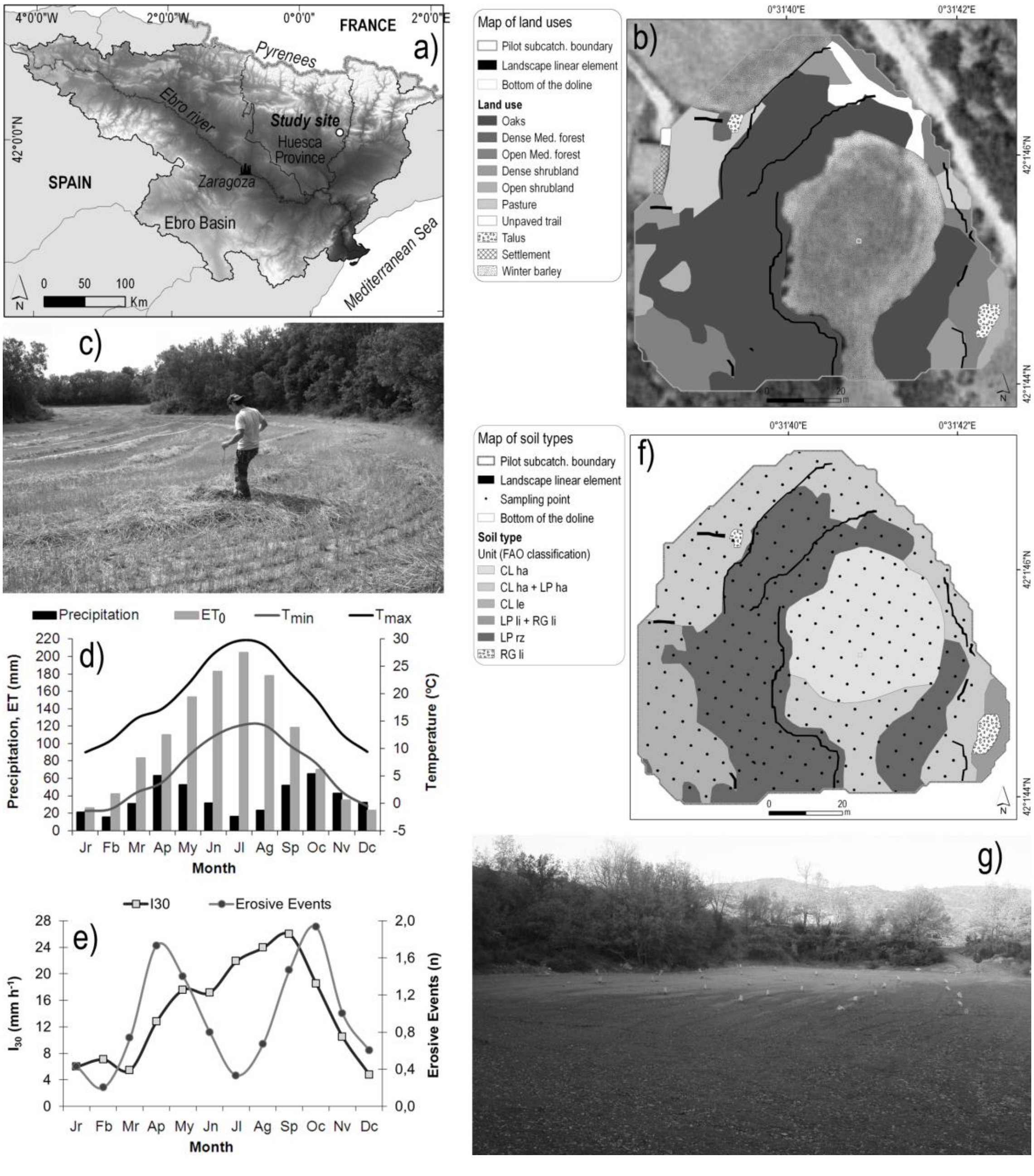

Figure 3 Map of the total annual runoff generated per raster cell (a) and monthly average runoff coefficients for the different soil types (b): *CLha*: Haplic Calcisol; *CLha+LPha*: Haplic Calcisol + Haplic Leptosol; *CLle*: Leptic Calcisol; *LPrz*: Rendzic Leptosol.

a)

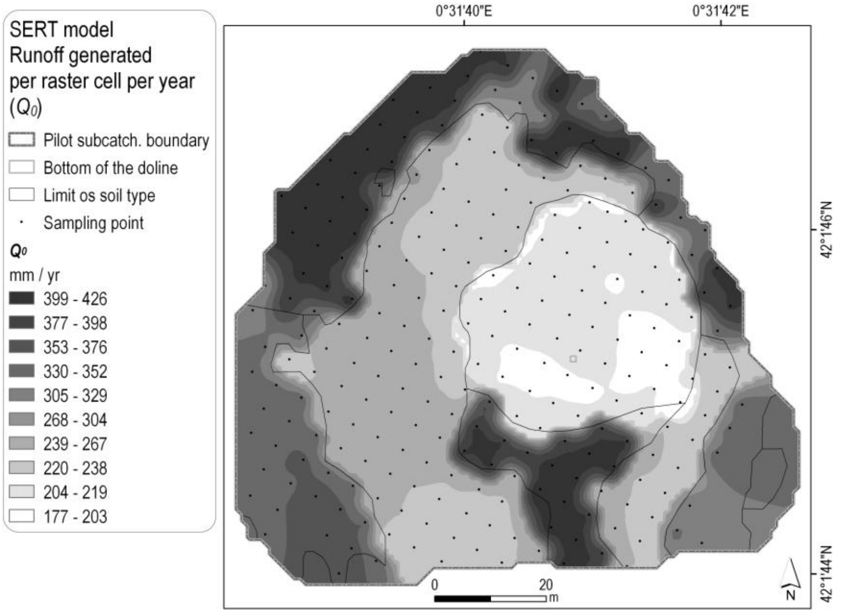

b)

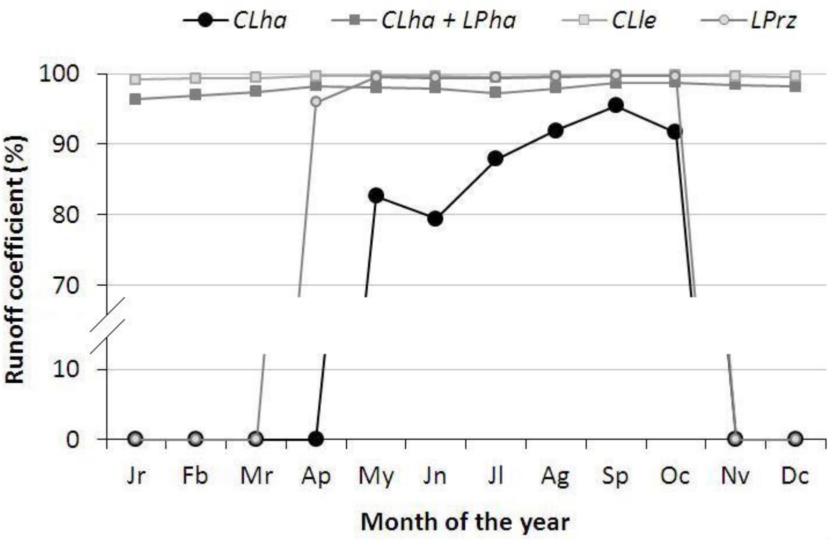

Figure 4 Map of average annual soil erosion (*SERT-Er*) at the *Pilot catchment* (a) and boxplots of the monthly rates of soil erosion at the soil sampling points (b). The Y axis of the boxplots are in logarithmic scale and horizontal lines represent the 10%, 25%, 50%, 75%, 90% and average values. All outliers are included.

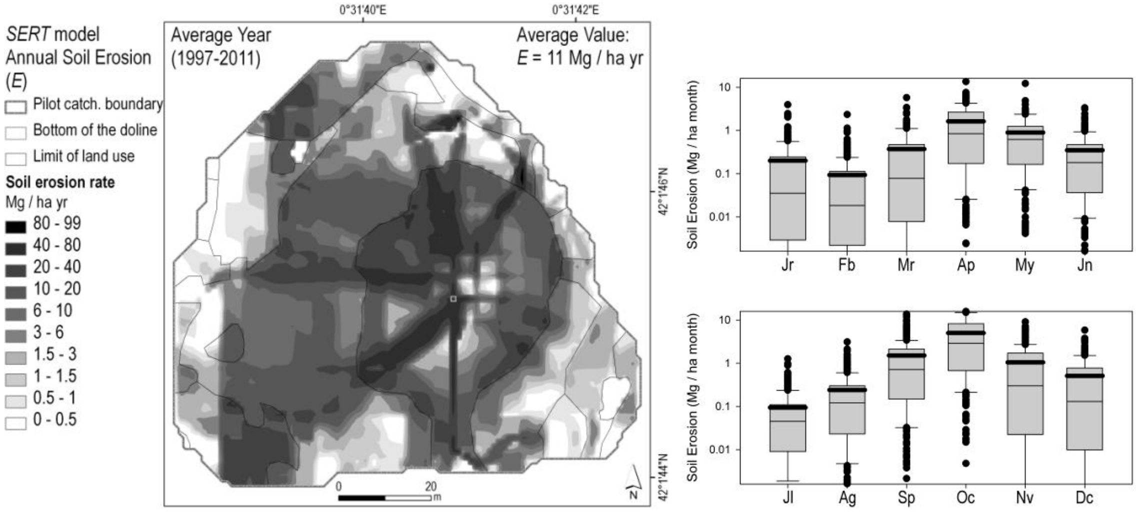

Table 2 Percentage of eroded area within each type of soil for each month of the year and mean and standard deviation values of predicted soil erosion with the *SERT* model. *CLha*: Haplic Calcisol; *CLha+LPha*: Haplic Calcisol + Haplic Leptosol; *CLle*: Leptic Calcisol; *LPrz*: Rendzic Leptosol.

Month	Soil type and number of soil samples											
	CL ha (*n*=58)			*CL ha* + *LP ha* (*n*=80)			*CL le* (*n*=26)			*LP rz* (*n*=102)		
	*%Ea**	*m***	*sd****	*%Ea*	*m*	*sd*	*%Ea*	*m*	*sd*	*%Ea*	*m*	*sd*
Jan	97.4	0.28	0.45	97.4	0.13	0.40	99.3	0.16	0.25	94.5	0.18	0.29
Feb	100.0	0.13	0.20	98.1	0.06	0.20	100.0	0.08	0.11	99.8	0.09	0.15
Mar	96.8	0.45	0.68	97.1	0.22	0.66	99.3	0.40	0.57	92.8	0.39	0.54
Apr	98.8	**2.25**	2.47	98.1	**0.89**	1.75	100.0	**2.04**	2.51	100.0	**1.62**	1.20
May	100.0	0.58	0.37	98.1	0.42	0.91	100.0	**1.36**	1.67	100.0	**1.25**	0.96
Jun	100.0	0.55	0.73	98.1	0.20	0.47	100.0	0.33	0.41	100.0	0.39	0.42
Jul	100.0	0.21	0.28	98.1	0.06	0.16	100.0	0.06	0.07	100.0	0.08	0.11
Aug	100.0	0.52	0.68	98.1	0.15	0.39	100.0	0.15	0.19	100.0	0.21	0.26
Sep	100.0	**3.02**	3.93	98.1	**0.88**	2.19	100.0	**1.31**	1.60	100.0	**1.31**	1.07
Oct	100.0	**11.15**	4.94	98.1	**4.22**	5.59	100.0	**2.78**	3.07	100.0	**2.20**	1.73
Nov	97.0	**1.91**	2.28	97.2	**0.70**	1.48	99.3	0.86	1.13	93.4	0.75	0.89
Dec	97.7	0.87	1.14	97.4	0.34	0.82	99.3	0.43	0.60	93.4	0.43	0.57
Year	100.0	21.92	16.01	98.1	8.27	12.88	100.0	9.96	11.60	100.0	8.88	7.12

%Ea: Percentage of eroded area; m**: mean value of soil erosion; and sd***: standard deviation value of soil erosion*

Figure 5 Maps of soil redistribution at the Pilot catchment for each month of the year estimated with the *SERT* model.

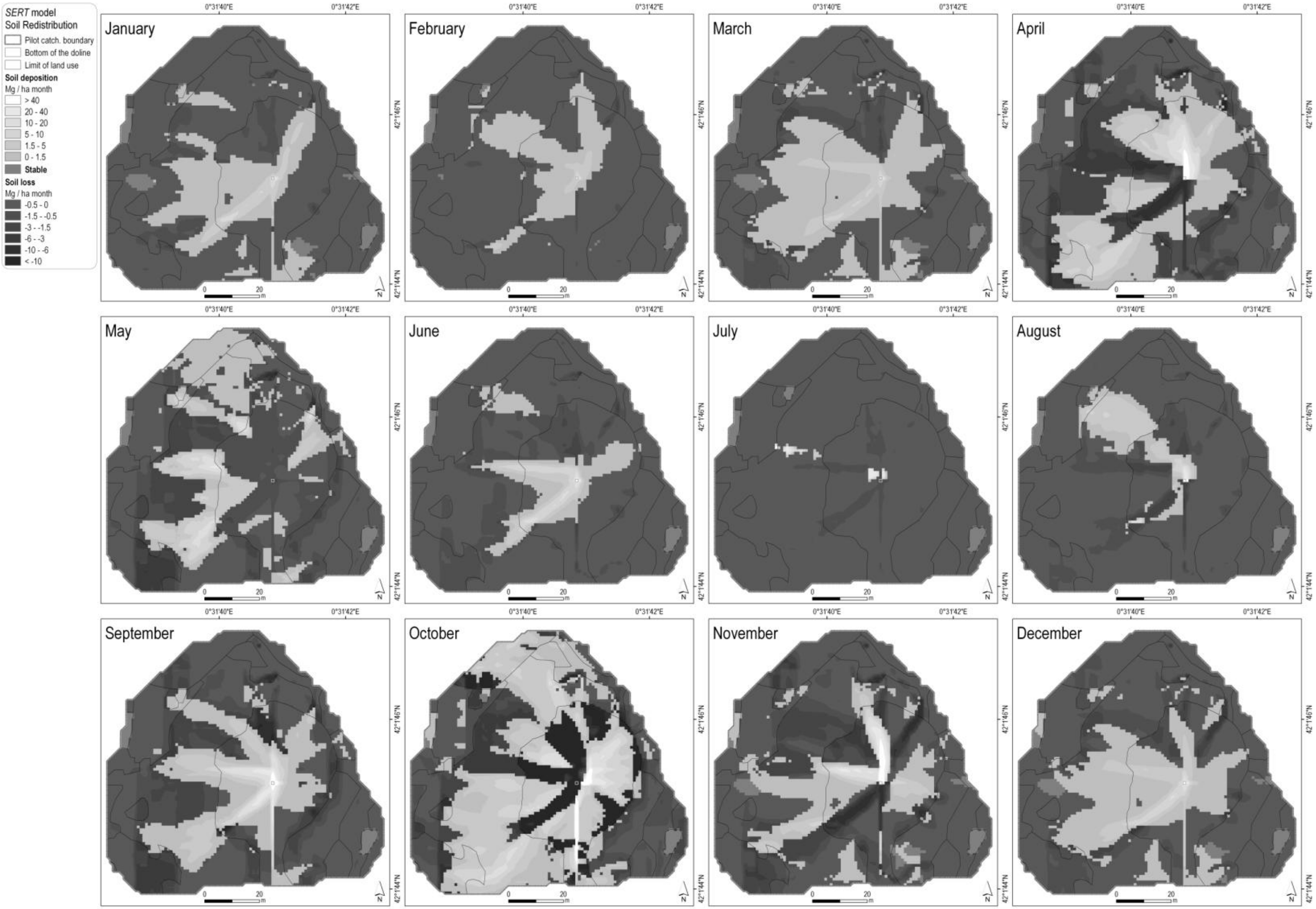

Figure 6 Map of average annual soil redistribution estimated with the *SERT* model (a) and correlation between predicted (*SERT-Rd*) and measured (^{137}Cs) values of soil loss and deposition (b). *LLE*: Landscape Linear Element.

a) b)

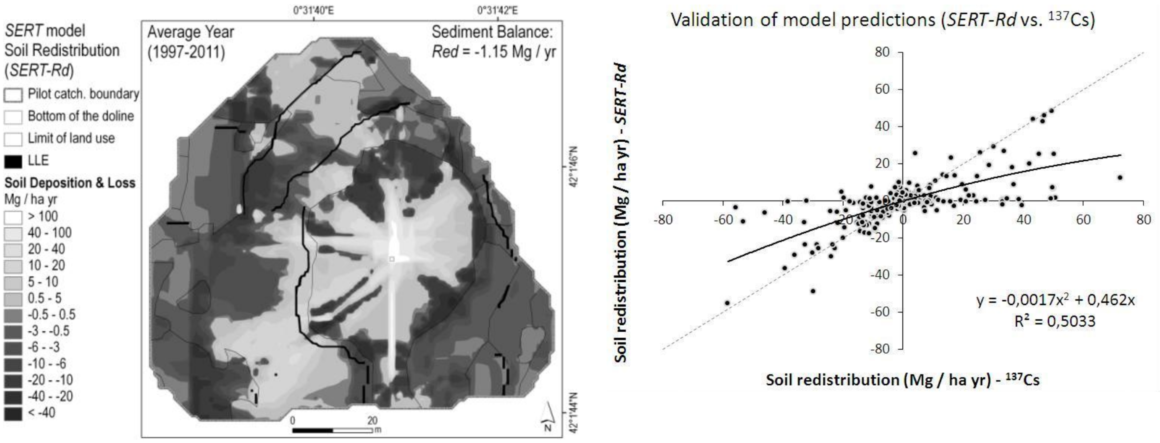

Table 3 Soil redistribution rates (in Mg ha^{-1} yr^{-1}) quantified with ^{137}Cs and predicted with the *SERT* model (*SERT-Rd* module) for the different land uses and in the control points.

Land use		^{137}Cs				*SERT-Rd*			
		n*	min	mean	max	n*	min	mean	max
Cultivated	Loss	19	1.9	29.4	63.9	48	0.1	10.9	36.3
	Dep.	26	0.4	24.8	136.5	43	0.2	13.4	48.3
Rangeland	Loss	41	0.1	9.4	107.4	111	0.1	4.7	55.3
	Dep.	46	0.2	7.8	178.9	57	0.1	3.3	13.5
	Stable	1	0.0	0.0	0.0	7	0.0	0.0	0.0
Total in Pilot sub-catchment	Loss	60	0.1	15.8	107.4	159	0.1	6.6	55.3
	Dep.	72	0.2	14.1	178.9	100	0.1	7.7	48.3
	Stable	1	0.0	0.0	0.0	7	0.0	0.0	0.0

n*: Number of control points in each land use